

Proceeding Paper

# $^{99m}\text{Tc}$ -Selenium-NPs as SPECT Tracer: Radio Synthesis and Biological Evaluation <sup>†</sup>

Akhilesh Kumar Singh <sup>1</sup>, Mohd. Faheem <sup>1,2</sup>, Amit Jaiswal <sup>1</sup>, Malleswari Ponnala <sup>3</sup>, Sanjay Gambhir <sup>1</sup>  
and Manish Dixit <sup>1,\*</sup>

<sup>1</sup> Department of Nuclear Medicine, Sanjay Gandhi Postgraduate Institute of Medical Sciences, Uttar Pradesh 226020, India; email1@email.com (A.K.S.); email2@email.com (M.F.); email3@email.com (A.J.); email5@email.com (S.G.)

<sup>2</sup> Department of Chemistry, University of Lucknow, Uttar Pradesh 226007, India

<sup>3</sup> Science Department, Borough of Manhattan, Community College, CUNY, New York, NY 10007, USA; email4@email.com

\* Correspondence: dixitm@sgpgi.ac.in

<sup>†</sup> Presented at the 27th International Electronic Conference on Synthetic Organic Chemistry, 15–30 November 2023; Available online: <https://ecsoc-27.sciforum.net/>.

**Abstract:** As the usage of nano-sized complexes in biomedical applications has grown significantly over the past ten years, nanoparticles are now playing a significant role in the enhancement and revolution of medical applications. It may be due primarily to the novel and exceptional electrical, optical, photoresponsive, and catalytic capabilities displayed by particles with sizes ranging from 1 to 100 nm. The radiolabelled nanoparticles refer to the process of incorporating radioactive isotopes into nanoparticles. This technique enables the nanoparticles to be tracked, imaged and monitored using various imaging techniques, such as Single-Photon Emission Computed Tomography (SPECT/CT) or Positron Emission Tomography (PET). They play a crucial role in understanding the biodistribution, pharmacokinetics, and targeted delivery of nanoparticles to biological systems. In this study, Selenium-based nanoparticles (SeNPs) were explored for imaging potential as these are usable due to their size, surface and kinetics, as well as their ability to be functionalized. The <sup>99m</sup>Technetium (<sup>99m</sup>Tc) radionuclide was used to radio labelled the bio-inspired highly dispersed grown over endophytic fungus *Fusarium oxysporum* selenium NP using conventional radio chemistry protocol. The radiolabeling yield was found  $94.5 \pm 3\%$  and analysed by various analytical tools. The synthesized <sup>99m</sup>Tc-SeNPs were assessed through in-vitro stability and their In-vivo biodistribution was performed. The accumulation post 6 hour data was primarily seen in the liver (around 3.4% ID/g) and lungs (about 2.2% ID/g). These SeNPs can be used as an imaging agent for lung and liver disorders because these NPs quickly pass through kidneys and get expelled via urine and shows long retention time in the body. These properties of <sup>99m</sup>Tc-SeNPs can be used for non-invasive imaging via SPECT.

**Keywords:** Nanoparticles; Radiolabelling; <sup>99m</sup>Tc; SPECT; Imaging

**Citation:** Singh, A.K.; Faheem, M.; Jaiswal, A.; Ponnala, M.; Gambhir, S.; Dixit, M.  $^{99m}\text{Tc}$ -Selenium-NPs as SPECT Tracer: Radio Synthesis and Biological Evaluation. *Chem. Proc.* **2023**, *14*, x. <https://doi.org/10.3390/xxxxx>

Academic Editor: Firstname  
Lastname

Published: 15 November 2023



**Copyright:** © 2023 by the authors. Submitted for possible open access publication under the terms and conditions of the Creative Commons Attribution (CC BY) license (<https://creativecommons.org/licenses/by/4.0/>).

## 1. Introduction

Nanotechnology in diagnostics via In-vivo research shows the enhancement the treatment of diseases [1]. This technology plays a dynamic role in pharmaceuticals that have been exploited in design of tumour-targeting agents that can be used for selective drug delivery, targeted hyperthermia treatment or specific imaging of tumour sites, resulting in improved therapy and diagnosis [2–4]. The nanopharmaceuticals used in the way of radiation to form radionanoparticles (such as SeNPs in this study) that can be used for imaging as well as therapy. In order to improve diagnostic outcomes and therapeutic effects in a number of diseases, the most significant of which being cancer, recent

advancements in nuclear medicine have been concentrated on the discovery and development of novel radiopharmaceuticals as theranostics. A radiopharmaceutical's effectiveness is influenced by the kind of carrier it contains and the radionuclide that is chelated or labelled with the moieties. The carrier could be an organic or inorganic molecule/nanoparticles such as selenium NPs that can accumulate on a particular diseased region to work therapeutically or diagnostically [5]. The radiopharmaceutical's thernostics properties are determined by the radionuclide's particle emission which is bounded with the carrier [6]. To achieve the desired outcome with the least amount of radiation exposure to healthy tissues, the optimum radiopharmaceutical should concentrate on the tumour area [7]. The optimum size and physical characteristics of Se-NPs make them particularly as radiopharmaceutical using radionuclides for molecular imaging. These characteristics enable improved kinetics and biological activities at subcellular levels. Additionally, the incorporation of a targeting molecule, such as a peptide or an antibody specific to a tumour, onto the surface of the selenium nanoparticle has significantly improved their ability to target, which was previously just a matter of perfusion due to the increased permeability and retention effect of the tumour vasculature [8]. The enormous surface area of selenium nanoparticles allows for further effective alterations, such as the attachment of imaging moieties, in addition to functionalizing them with targeted ligands [9]. The synthesis of  $^{99m}\text{Tc}$  based nanoparticle labelling represents a significant advancement in the field of nuclear medicine and nanotechnology. These nanoparticles are modified using  $^{99m}\text{Tc}$ , a radioisotope with ideal properties for medical imaging for diagnosis due to its ideal half-life and minimal radiation exposure [10–12]. The synthesis process involves precise control over the size, shape, and surface properties of the nanoparticles, ensuring their stability and biocompatibility [13]. Once synthesized, these  $^{99m}\text{Tc}$  labelled nanoparticles find versatile applications in the medical field. They are commonly used as highly efficient and targeted imaging agents for various diseases, including cancer, cardiovascular disorders, and neurodegenerative conditions [14]. Their small size allows them to navigate through the body, reaching specific cells or tissues of interest. Moreover, their radioactive properties enable precise imaging, aiding clinicians in accurate diagnosis and treatment planning. Additionally, ongoing research explores the potential of these nanoparticles in assessing the therapeutic response of targeted radiotherapy, promising a future where these innovative nanoparticles could revolutionize the landscape of personalized medicine and patient care [15–17]. The majority of selenium nanoparticles have limited blood circulation time, enhanced toxicity and are subjected to rapid uptake by the reticuloendothelial system in vivo [18]. The syntheses of nanoparticles via chemical methods are very common but this method having issues e.g. use of excess solvent and other harmful chemicals [19]. The overcome this problem adopted biosynthesized nanoparticles which are highly stable, water-soluble and capped by phytochemicals or natural protein molecules. In this article, our group successfully radiolabelling nanoparticles, which are isolated from biological processes and labelled them with  $^{99m}\text{Tc}$  radionuclide. And explored these tracers as non-invasive imaging tools for various biological disorders.

## 2. Material and Methods

All the chemicals and reagents were used of analytical reagent grade and utilized without further purification. The selenium tetrachloride ( $\text{SeCl}_4$ ) was used for the biosynthesis of Se-NPs, purchased from Sigma-Aldrich India Pvt. Ltd. The Technetium-99m was eluted from  $^{99}\text{Mo}/^{99m}\text{Tc}$  generator as pertechnetate (SDS Life Sciences Pvt. Ltd., India). Instant thin-layer chromatography paper (iTLC) was purchased from Sigma Aldrich (India Pvt. Ltd.). The radiolabeling was conformed by rTLC (Eckert and Ziegler Radiopharma, MiniScan PRO, USA, 61-20-0) using PMT based Detector B-FC-3200, 660V was used for determination of purity of radiopharmaceuticals. The radioactive samples were analyzed using a NaI (TI)  $\gamma$ -ray scintillation counter (CAPTUS<sup>®</sup> 3000 gamma counter CAPINTEC, Ramsey, NJ, USA).

### 2.1. Biosynthesis of Se-NPs

As already documented in the literature by Abasar et al. [20], in brief, the synthesis of SeNPs, about 20 grams of biomass were added to 100 mL of newly made aqueous  $\text{SeCl}_4$  solution (2 mM) in 500 mL Erlenmeyer flask (sterilized) for the biosynthesis of Se-NPs. The reaction was preceded at room temperature and put on the shaker (~200 rpm). The mycelia were removed from the appropriate medium by a straightforward filtration process after 72 h the reaction had been completed. After of preparation, the Se-NPs was lyophilized or dried. The synthesized Se-NPs were characterized by using different techniques like FTIR, UV-Vis spectrophotometer, TEM and XRD.

### 2.2. Radiolabeling of Selenium Nanoparticles

The radiolabeling synthesis was carried out in a V-shaped vial. The radiolabeling procedure of Se-NPs with  $^{99m}\text{Tc}$  was adopted in the reported literature [21] with slight modification. The Se-NPs were added in a dry & clean V-shaped vial and added 100  $\mu\text{L}$  (200–370 MBq) of a fresh elute  $^{99m}\text{Tc}$  as  $\text{Na}^{99m}\text{TcO}_4$  in saline solution, Figure 1. The V-shape vial was stirred at 40 °C.

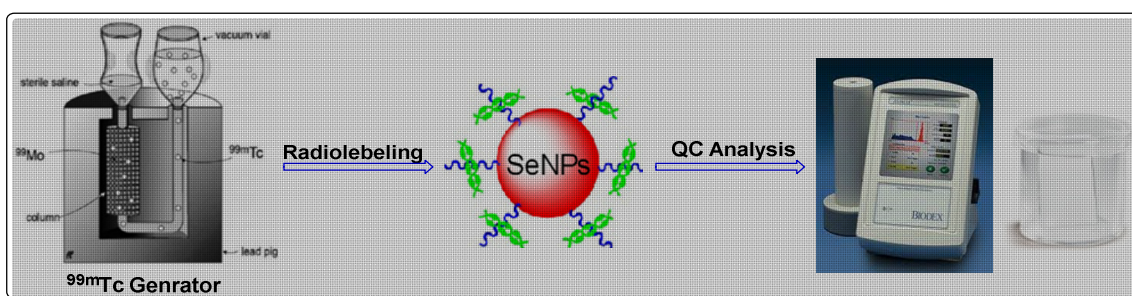


**Figure 1.** Systematic synthesis of radiolabel Se-NPs with  $^{99m}\text{Tc}$  radionuclide.

### 2.3. Radiochemical Yield of [ $^{99m}\text{Tc}$ ]TcSe-NPs

The Instant Thin layer Chromatography (iTLC), 12 cm long and 1 cm wide was used for the radio-chemical yield (RCY) of radiolabeled Se-NPs. The Silica based TLC plate marked at a distance of 2 cm from the lower end and lined into sections 1 cm each up to 10 cm. After of reaction, a drop of the reaction mixture was spotted on the TLC stripe and developed in acetone as a developing solvent. After developing, the TLC cut into two pieces of 1 cm each. The sections were then counted using a NaI (TI)  $\gamma$ -ray scintillation counter to determine the radiochemical yield (RCY). To calculate the percentage of RCY, the radioactivity of radiolabeled nanoparticles [ $^{99m}\text{Tc}$ ]Tc-Se-NPs was divided by the total activity and multiplied by 100. The radiolabeling efficiency with Se-NPs was in the range of >95%, and stability was evaluated at various time scales under physiological solutions and conditions.

### 2.4. In-Vivo Biological Studies

All animal experiments were conducted in compliance with Committee for Control and Supervision of Experiment on Animal (CCSEA) and with approval of institutional ethics committee (Reference No.: SGPGIMS/AH/24th IAEC/P-20/084/2018). For In-vitro evaluation a group of healthy Wistar rats were used for the evaluation of [ $^{99m}\text{Tc}$ ]Tc-SeNPs at various time intervals. The [ $^{99m}\text{Tc}$ ]Tc-SeNPs complex, 75  $\mu\text{L}$  (11–14 MBq) NP solution was intravenous (I.V.) injected in the tail vein of rat. After imaging, rats were sacrificed and their organs were removed, washed with saline, weighed, and measured their radioactivity using gamma counter. The following formula was used to calculate the proportion of the administered dose per gram of tissue (%ID/g), and the tissue uptakes were assessed.

$$\%ID/g = \frac{\text{Counts per gram of organ}}{\text{Counts dose given (total)}} \times 100$$

### 3. Results and Discussion

The  $^{99m}\text{Tc}$ -radionuclides have versatile chemistry, which has been exploited for the labelling of biomolecules. Technetium is the 43rd element in the periodic table and belongs to the group of transition metals owing to its electronic configuration of  $[\text{Kr}]4d^55s^2$ . Technetium provides several opportunities for complex formation with a large number of different ligands due to its oxidation state (OS) varying from +1 up to +7. The structure of technetium complexes can also be characterized by the coordination number ( $N$ ), which can vary from 4 to 7. The typical approach employed in the synthesis of first-generation radiopharmaceuticals in the past was direct labelling through the reduction of pertechnetate with stannous chloride in an acidic environment. The labelling of Se-NPs was optimized under reduction using 0.1 mg of  $\text{SnCl}_2 \cdot \text{H}_2\text{O}$  as a reducing agent as documented in the literature with slight modification. The various concentrations of nanoparticles were explored for radio-labeling and the best yield was obtained when the concentration of the NPs was in the range of 35–40  $\mu\text{g}$ .

The stability of the radiolabeled nanoparticles is shown in Figure 2a,b, respectively, while the chelation stability was maintained in physiological saline and human serum albumin solutions. The stability was evaluated by using the iTLC method at various time points as shown in Figure 2. The data shows that stability retains till 350 min in saline whereas 1140 min in albumin. The resulting outcome shows that the Se-NPs were superbly chelated with the metallic radionuclide ( $^{99m}\text{Tc}$ ) at physiological pH range or at environment containing human serum albumin.

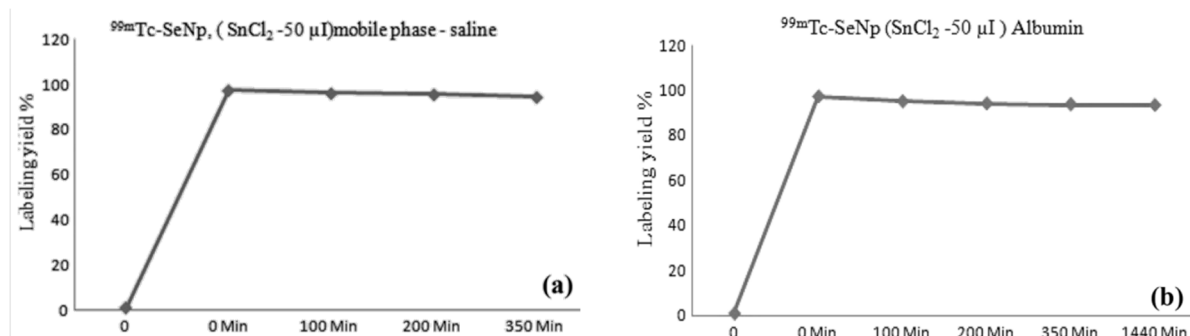


**Figure 2.** Stability study of  $^{99m}\text{Tc}$ ]TcSe-NPs at different time intervals at (a) in saline (b) in albumine at 37 °C.

For biodistribution studies the  $^{99m}\text{Tc}$ ]TcSe-NPs complex was injected through tail vein (11–14 MBq) and mice were imaged at respective time scale and scarified to calculate the biodistribution radioactivity in different organ of interest.

The maximum percentage injected dose per gm organ (% ID/g) of  $^{99m}\text{Tc}$ ]TcSe-NPs complex in the liver was  $19.47 \pm 4\%$  at 10 min post-injection (p.i.) with no significant accumulation in the spleen, but the accumulation also shows in lungs and stomach with the range of  $6 \pm 1\%$  and  $9.4 \pm 2$  at 10 min p.i., which is indicating that radiolabeled nanoparticle is well distributed (Figure 3).

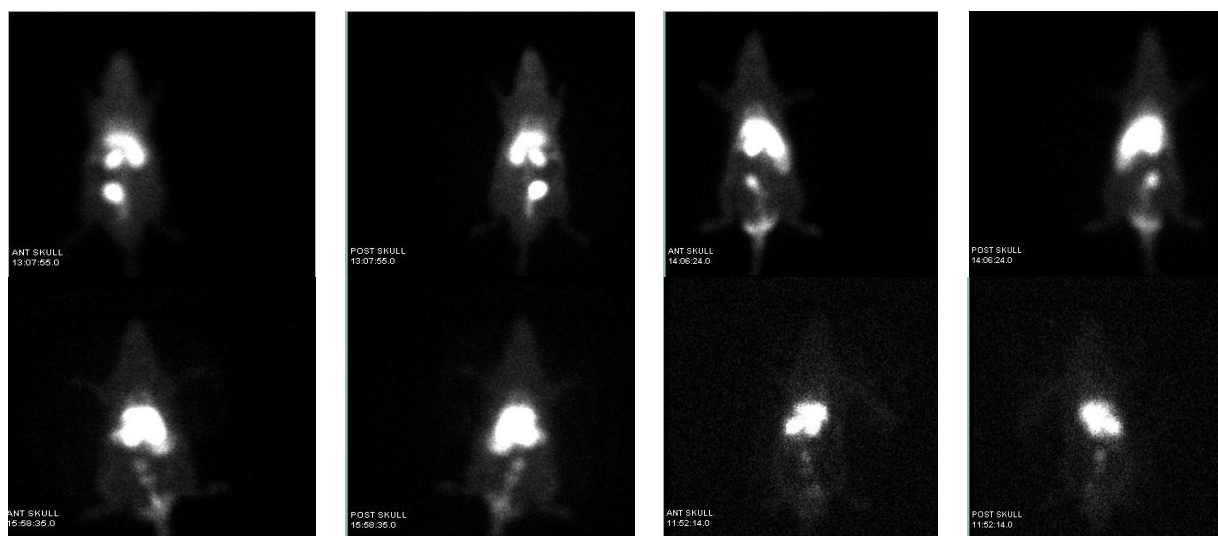


Figure 3. SPECT based imaging of  $[^{99m}\text{Tc}]\text{TcSe-NPs}$  in Wister Rat.

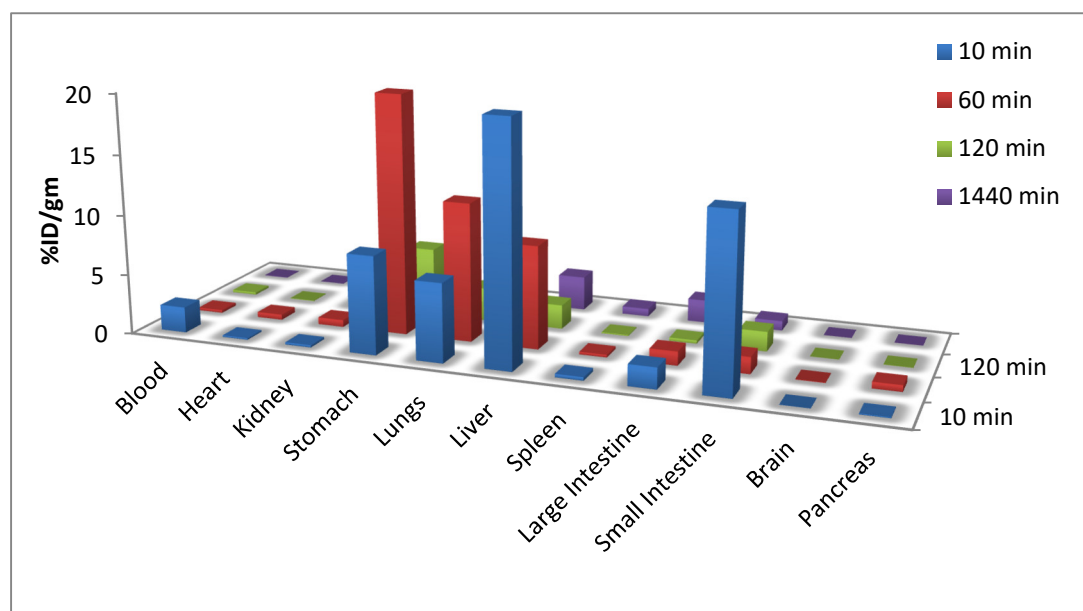


Figure 4. Biodistribution of  $[^{99m}\text{Tc}]\text{TcSe-NPs}$  in Wister Rat organ.

According to the data, these radiolabeled nanoparticles are much larger than the hydrodynamic diameters (HDs) of the renal clearance threshold, which is  $<6$  to  $8$  nm. The kidney's activity at around  $3.8 \pm 2$  after 6 hours post-injection revealed that nanoparticles were being excreted through the urinary system. The investigation at post 6 h revealed mostly accumulation in the liver and lungs (at  $3.4\%$  ID/g and  $2.2\%$  ID/g, respectively), which is suggestive of the nanoparticles' particle size. These nanoparticles could help with liver or lung disease. The Se-NPs have the benefit of having rapid blood circulation and enabling passive targeting via enhanced permeability and retention (EPR) effect. In addition, the nanoparticle can actively target the liver and lungs through molecular interaction or affinity, which will be helpful in evaluating the functionality of these organs.

#### 4. Conclusions

In conclusion, in this work, the size, surface, kinetics and capacity for functionalization, of selenium-based nanoparticles (Se-NPs) are examined and their imaging as radio-tracers. A conventional radiochemistry approach was utilized to radio-label the naturally isolated Se-NPs with the  $^{99m}\text{Tc}$  radionuclide with  $94.5 \pm 3\%$ , radiolabeling yield and examined using several analytical techniques. The stability of the synthesized [ $^{99m}\text{Tc}$ ]TcSe-NPs was assessed in vitro and their biodistribution was carried out in vivo across a wistar rat at several time points. The experiment conducted at post 6 hours revealed an accumulation that was concentrated mostly in the liver (about 3.4% ID/g) and lungs (around 2.2% ID/g), which is suggestive of the nanoparticles' particle size. This characteristic of these [ $^{99m}\text{Tc}$ ]TcSe-NPs makes them useful for SPECT imaging as non-invasive biomarkers. Further exploration of these kinds of nanoparticles is underway to enhance their kinetics and clearance profile.

**Funding:** This research received no external funding.

**Acknowledgments:** We are sincerely thankful to Aabsar Ahamd, Interdisciplinary Nanotechnology Centre (INC), AMU, Aligarh for providing Se-NPs. also to Atul K. Baranwal for their assistance with animal experiments.

**Conflicts of Interest:** The authors declare no conflict of interest.

#### References

1. Chen, Y.; Chen, H.; Shi, J. In vivo bio-safety evaluations and diagnostic/therapeutic applications of chemically designed mesoporous silica nanoparticles. *Adv. Mater.* **2013**, *25*, 3144–3176.
2. Wu, M.; Huang, S. Magnetic nanoparticles in cancer diagnosis, drug delivery and treatment. *Mol. Clin. Oncol.* **2017**, *7*, 738–746.
3. Babu, A.; Templeton, A.K.; Munshi, A.; Ramesh, R. Nanoparticle-based drug delivery for therapy of lung cancer: Progress and challenges. *J. Nanomater.* **2013**, *2013*, 14.
4. Van Vlerken, L.E.; Amiji, M.M. Multi-functional polymeric nanoparticles for tumour-targeted drug delivery. *Expert Opin. Drug Deliv.* **2006**, *3*, 205–216.
5. Weingart, J.; Vabbilisetty, P.; Sun, X.L. Membrane mimetic surface functionalization of nanoparticles: Methods and applications. *Adv. Colloid Interface Sci.* **2013**, *197*, 68–84.
6. Liu, S. Bifunctional coupling agents for radiolabeling of biomolecules and target-specific delivery of metallic radionuclides. *Adv. Drug Deliv. Rev.* **2008**, *60*, 1347–1370.
7. Sgouros, G.; Bodei, L.; McDevitt, M.R.; Nedrow, J.R. Radiopharmaceutical therapy in cancer: Clinical advances and challenges. *Nat. Rev. Drug Discov.* **2020**, *19*, 589–608.
8. Sun, T.; Zhang, Y.S.; Pang, B.; Hyun, D.C.; Yang, M.; Xia, Y. Engineered nanoparticles for drug delivery in cancer therapy. *Angew. Chem. Int. Ed.* **2014**, *53*, 12320–12364.
9. Veischi, O.; Gunn, J.W.; Zhang, M. Design and fabrication of magnetic nanoparticles for targeted drug delivery and imaging. *Adv. Drug Deliv. Rev.* **2010**, *62*, 284–304.
10. Roy, I.; Krishnan, S.; Kabashin, A.V.; Zvestovskaya, I.N.; Prasad, P.N. Transforming nuclear medicine with nanoradiopharmaceuticals. *ACS Nano* **2022**, *16*, 5036–5061.
11. Maccora, D.; Dini, V.; Battocchio, C.; Fratoddi, I.; Cartoni, A.; Rotili, D.; Castagnola, M.; Faccini, R.; Bruno, I.; Scotognella, T.; et al. Gold nanoparticles and nanorods in nuclear medicine: A mini-review. *Appl. Sci.* **2019**, *9*, 3232.
12. Pijera, M.S.O.; Viltres, H.; Kozempel, J.; Sakmár, M.; Vlk, M.; İlem-Özdemir, D.; Ekin, M.; Srinivasan, S.; Rajabzadeh, A.R.; Ricci-Junior, E.; et al. Radiolabeled nanomaterials for biomedical applications: Radiopharmacy in the era of nanotechnology. *EJNMMI Radiopharm. Chem.* **2022**, *7*, 8.
13. Bharti, C.; Nagaich, U.; Pal, A.K.; Gulati, N. Mesoporous silica nanoparticles in target drug delivery system: A review. *Int. J. Pharm. Investig.* **2015**, *5*, 124.
14. Varani, M.; Campagna, G.; Bentivoglio, V.; Serafinelli, M.; Martini, M.L.; Galli, F.; Signore, A. Synthesis and biodistribution of  $^{99m}\text{Tc}$ -labeled PLGA nanoparticles by microfluidic technique. *Pharmaceutics* **2021**, *13*, 1769.
15. Eldin, S.S.E.; Rashed, H.M.; Hassan, A.H.; Salem, H.F.; Sakr, T.M. Multifunctional  $^{99m}\text{Tc}$ -5-azacitidine Gold Nanoparticles: Formulation, In Vitro Cytotoxicity, Radiosynthesis, and In Vivo Pharmacokinetic Study. *Curr. Drug Deliv.* **2023**, *20*, 387–399.
16. Türker, S.; Özer, A.Y. Radiopharmacology and pharmacokinetic evaluation of some radiopharmaceuticals. *FABAD J. Pharm. Sci.* **2005**, *30*, 204.
17. Nokkaew, N.; Sliiratori, S.; Gonlachanvit, S.; Chaiwatanarat, T.; Nasing, T.; Chaiseri, S.; Sirisansaneeyakul, S.; Kaniuigsukkasem, V. Evaluation of the First Radiolabeled  $^{99m}\text{Tc}$ -Jerusalem Artichoke-Containing Snack Bar on Gastric Emptying and Satiety in Healthy Female Volunteers. *J. Med. Assoc. Thail.* **2018**, *101*.

18. Feng, Q.; Liu, Y.; Huang, J.; Chen, K.; Huang, J.; Xiao, K. Uptake, distribution, clearance, and toxicity of iron oxide nanoparticles with different sizes and coatings. *Sci. Rep.* **2018**, *8*, 2082.
19. Duan, H.; Wang, D.; Li, Y. Green chemistry for nanoparticle synthesis. *Chem. Soc. Rev.* **2015**, *44*, 5778–5792.
20. Mansouri-Tehrani, H.A.; Keyhanfar, M.; Behbahani, M.; Dini, G. Synthesis and characterization of algae-coated selenium nanoparticles as a novel antibacterial agent against *Vibrio harveyi*, a *Penaeus vannamei* pathogen. *Aquaculture* **2021**, *534*, 736260.
21. Snehalatha, M.; Venugopal, K.; Saha, R.N.; Babbar, A.K.; Sharma, R.K. Etoposide loaded PLGA and PCL nanoparticles II: Bio-distribution and pharmacokinetics after radiolabeling with Tc-99m. *Drug Deliv.* **2008**, *15*, 277–287.

**Disclaimer/Publisher's Note:** The statements, opinions and data contained in all publications are solely those of the individual author(s) and contributor(s) and not of MDPI and/or the editor(s). MDPI and/or the editor(s) disclaim responsibility for any injury to people or property resulting from any ideas, methods, instructions or products referred to in the content.